

Identifying Electrocardiogram Abnormalities Using a Handcrafted-Rule-Enhanced Neural Network

Yuxin Bian, Jintai Chen, Xiaojun Chen,

Xiaoxian Yang*, Danny Z. Chen, *Fellow, IEEE*, Jian Wu*, *Member, IEEE*

Abstract—A large number of people suffer from life-threatening cardiac abnormalities, and electrocardiogram (ECG) analysis is beneficial to determining whether an individual is at risk of such abnormalities. Automatic ECG classification methods, especially the deep learning based ones, have been proposed to detect cardiac abnormalities using ECG records, showing good potential to improve clinical diagnosis and help early prevention of cardiovascular diseases. However, the predictions of the known neural networks still do not satisfactorily meet the needs of clinicians, and this phenomenon suggests that some information used in clinical diagnosis may not be well captured and utilized by these methods. In this paper, we introduce some rules into convolutional neural networks, which help present clinical knowledge to deep learning based ECG analysis, in order to improve automated ECG diagnosis performance. Specifically, we propose a Handcrafted-Rule-enhanced Neural Network (called HRNN) for ECG classification with standard 12-lead ECG input, which consists of a rule inference module and a deep learning module. Experiments on two large-scale public ECG datasets show that our new approach considerably outperforms existing state-of-the-art methods. Further, our proposed approach not only can improve the diagnosis performance, but also can assist in detecting mislabelled ECG samples. Our codes are available at https://github.com/alwaysbyx/ecg_processing.

Index Terms—ECG classification, deep learning, rule inference

I. INTRODUCTION

ELECTROCARDIOGRAM (ECG) is a type of commonly-used test in clinical practice for diagnosing patients suffered from cardiac abnormalities. Over 300 million ECG records are produced worldwide each year [1], which are a heavy burden for manual ECG diagnosis. For example, in China, around 250 million individuals take ECG tests each year, but only around 36,000 proficient doctors are engaged in analyzing such ECG data [2]. Thus, there is a clear gap between the supply and demand in clinical ECG diagnosis.

Yuxin Bian and Jintai Chen are with the College of Computer Science and Technology, Zhejiang University, Hangzhou, 310027, China (e-mails: alwaysbyx@gmail.com, jtchen721@gmail.com).

Xiaojun Chen is with the RealDoctor AI Research Centre, Zhejiang University, Hangzhou, 310000, China. (e-mail: chenxiaojun@zju.edu.cn)

Xiaoxian Yang is with the School of Computer and Information Engineering, Shanghai Polytechnic University, China (e-mail: xyyang@sspu.edu.cn).

Danny Z. Chen is with the Department of Computer Science and Engineering, University of Notre Dame, Notre Dame, IN 46556, USA (e-mail: dchen@nd.edu).

Jian Wu is with the Second Affiliated Hospital School of Medicine and School of Public Health, Zhejiang University, Hangzhou 310058, China (e-mail: wujian2000@zju.edu.cn).

*Corresponding authors.

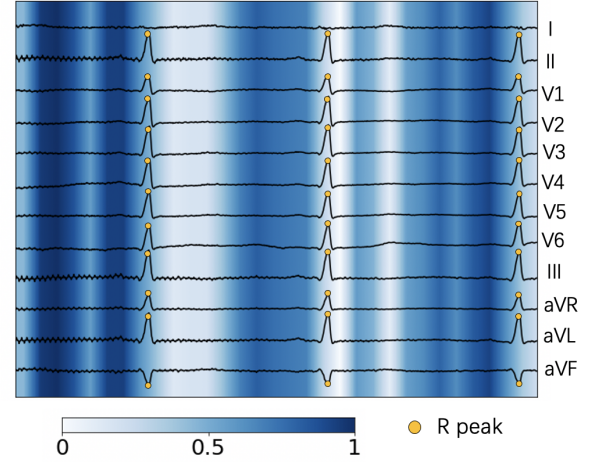


Fig. 1: Illustrating a saliency heat map for a case belonging to Counterclockwise Rotation (CCR, a type of cardiac abnormality). The ECG segments of interest are obtained by 1D ResNet-34 with Grad-CAM [3], and are visualized after being scaled with importance and normalized to 0–1. Yellow dots refer to the R peaks of ECG.

Recently, artificial intelligence (AI) methods have been revolutionizing various tasks [4]–[8], including diagnosis practices [9]–[14] and provided effective assistance in automated signal analysis. Compared with doctors’ (manual) analysis of ECG, such methods can make cardiac abnormality diagnosis more efficient. Among them, many machine learning methods were proposed for automated ECG diagnosis. In early years, various traditional methods employing decision trees [15], SVM [16], random forests [17], and Bayesian networks [18] were applied to classify ECG signals, but did not yield satisfactory performances. Recently, deep learning approaches have drastically improved performances of various recognition tasks, including automatic ECG diagnosis [10], [13], [19]–[22]. Deep learning methods for ECG can be roughly divided into three types, graph based [23]–[25], recurrent neural network (RNN) based [26]–[28], and convolution based [13], [14], [21], [29] methods. Specifically, graph based neural networks aim to capture the dependencies among cardiac abnormalities, since many ECG cases belong to multiple categories (abnormality types). RNN based methods treat ECG signals as time series and perform temporal feature extraction. Convolution based methods process ECG data as a special case of images, and often achieve better results [21].

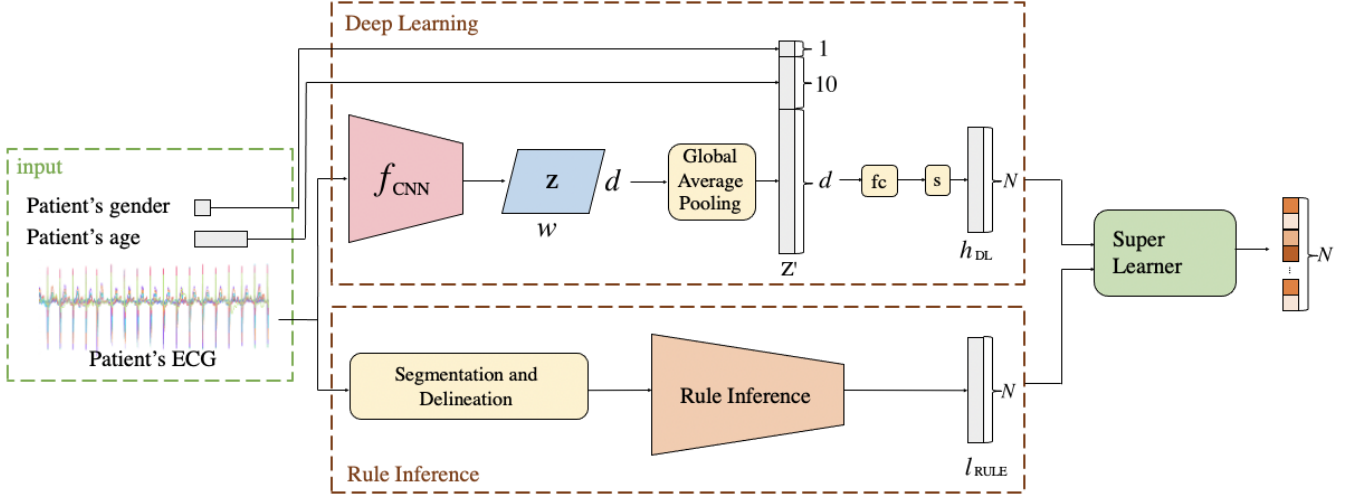


Fig. 2: The overall framework of our HRNN for multi-label ECG abnormality classification. N denotes the types of abnormalities. We transform the patient's gender and age into a scalar and a vector of size 10, respectively, and concatenate them with the final d -dimensional feature vector extracted by the CNN with the global average pooling operation ("fc" indicates a fully-connected layer and "s" indicates a sigmoid layer).

In clinical practice, clinicians often analyze ECG records in two main aspects: (1) experienced doctors may analyze whether the shapes of some key segments are normal, including P waves, T waves, and QRS complexes; (2) clinicians quantitatively analyze voltages and duration of certain waves. However, the existing neural network based methods do not seem to be able to capture the key segment voltages well. For example, we performed a classification study on ECG signals, and observed some inconsistency between the segments taken seriously by clinicians and those by neural networks. An example for this is given in Fig. 1. A clinical diagnostic criterion for the Counterclockwise Rotation (CCR) abnormality is to identify the presence of an R peak shift in the lead V1-V6. In Fig. 1, the blue parts mark the critical segments of a CCR case obtained by a trained 1D ResNet-34 [4] with the Grad-CAM approach [3]. One can see that the 1D ResNet-34 does not even focus on the R peaks (as marked in Fig. 1), which is obviously not consistent with the clinical criterion for CCR. Similar inconsistency can be found on detecting other abnormalities on ECG. For a specific abnormality, clinicians can determine whether it presents by analyzing the corresponding key segment (e.g., an ST segment), but neural network based methods may give weights to every point in an ECG signal and do not even care about the key segment focused by clinicians.

To address this issue, we resort to introducing some clinical knowledge for detecting cardiac abnormalities into deep neural networks, and develop a new method, called **Handcrafted-Rule-enhanced Neural Network (HRNN)**, to improve ECG classification accuracy. In this work, some critical information for ECG classification (e.g., the voltage of R peak, the interval of Q wave) is provided by some handcrafted rules to deal with the drawbacks of known neural networks. HRNN, for ECG classification with standard 12-lead ECG input, consists of a rule inference module and a deep learning module.

To combine the rule-based method and deep learning based method, HRNN treats both of them as meta learners, and employs a super learner to combine their predictions.

We evaluate HRNN on two large-scale public ECG datasets for multi-label classification of 34 and 55 kinds of abnormalities, respectively. Comprehensive experiments demonstrate the superior performances of HRNN for cardiac abnormality detection in comparing with state-of-the-art methods. In a case study, the results suggest that our proposed model can be applied to detect mislabeled samples, which can help improve the annotation accuracy of ECG datasets.

The major contributions of this work are as follows:

- We construct a rule-enhanced module to help promote neural networks, by providing rules according to diagnostic knowledge for ECG analysis. This design aims to provide clinical interpretation for arrhythmia with a higher consistency with experts' attention on ECG.
- Our model surpasses current state-of-the-art methods on two large-scale public ECG classification datasets, verifying the effectiveness of the handcrafted rules we use.
- In a case study, we show that our model is able to assist in detecting mislabeled samples, which is possibly beneficial to some practical tasks including corrupted label correction and AI-assisted annotation.

II. RELATED WORK

Automated diagnosis has recently witnessed a rapid progress due to the fast development of deep neural networks (DNNs). In particular, many efforts have been dedicated to extending deep neural networks and designing DNN models for ECG classification. Hannun et al. [21] first developed a DNN to classify 12 arrhythmia classes and demonstrated that an end-to-end DNN can classify a broad range of distinct arrhythmias from single-lead ECGs with high diagnostic

performance. Many improvements were based on it. Wang et al. [23] added graph attention networks to capture class dependencies. Luo et al. [22] combined bi-directional long short term memory (LSTM) with DNN to capture temporal features, dividing ECG data into 9 classes. However, these methods did not take into account whether a DNN correctly focuses on the key information in ECG signals to detect the corresponding classes, which might yield inferior performance in identifying some diseases.

On the other hand, many researchers attempted to utilize clinical knowledge in automated ECG analysis. Zhang et al. [30] proposed a disease-specific feature selection method to select ECG features and classify ECGs into five types. Xu et al. [31] used handcrafted rules in morphological classification for ST segments, and obtained more detailed and better results than the previous neural network methods [32], suggesting possible clinical significance. Jin et al. [33] combined a rule inference method and a convolutional neural network (CNN) to classify ECG data into normal and abnormal classes; they used some statistics (mean and variances) to depict the heart rate for diagnosis. Sannino et al. [34] detected peaks and waves to extract ECG temporal features, and leveraged a neural network to classify normal and abnormal ECG cases. In [35], Mondéjar et al. used support vector machine (SVM) to cope with temporal and morphological information (e.g., RR intervals of ECGs, wavelets, and several amplitude values). However, they simply constructed some rules or fed hand-crafted features to the models, resulting in sub-optimal performances. We argue that it would be more effective to combine rule-based features and neural networks. In addition, these methods were only presented to classify limited types of abnormalities (binary classification in most cases) and could not identify multiple diseases simultaneously, which did not meet the needs in clinical practice.

Compared with the aforementioned methods, our proposed method does not simply feed ECG features to classifiers. In contrast, we construct different rules for different abnormalities based on clinical knowledge, and fuse the rule-based outputs and multi-label predictions of a deep learning model.

III. METHODOLOGY

In clinical practice, clinicians often analyze ECG signals by focusing on certain particular segments when determining whether specific abnormalities are observed. For instance, an ECG signal is determined to be a case of “low QRS voltage” if the amplitudes of all the QRS complexes in the limb leads are < 0.5 mV, and the amplitudes of all the QRS complexes in the precordial leads are < 1.0 mV. Deep neural networks have been shown to have advantages in capturing shape patterns, leading to breakthroughs in image recognition. Also, motivated by clinical practice, we think rule-based methods can well complement deep neural networks for ECG analysis.

Based on the above motivation, we design a new handcrafted-rule-enhanced neural network (HRNN) for identifying ECG abnormalities (see Fig. 2 for an overview of HRNN). We seek to leverage the power of a convolutional neural network (CNN) for automatic feature extraction, while

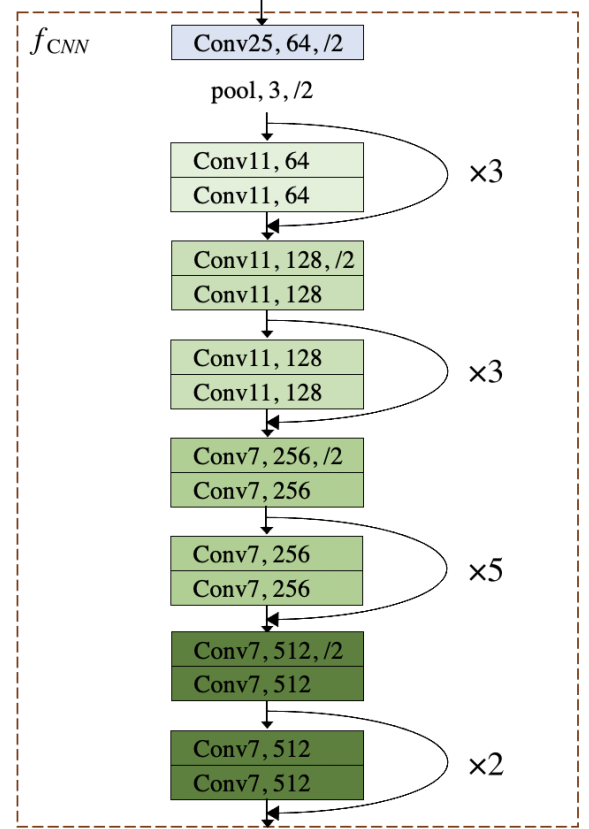


Fig. 3: Our f_{CNN} architecture. Different from ResNet-34 [4], we use 1D convolution operation since we treat the input ECG as 1-dimensional signals. “Conv i, j ” represents a convolutional layer with j kernels of size i . If followed by “/2”, it represents a convolutional layer with stride 2. “Pool, 3, /2” indicates a maxpool layer with kernel size 3 and stride 2. “ $\times n$ ($n \in \{2, 3, 5\}$)” indicates that the residual block repeats n times in sequence.

employing a rule-based module to provide some key information that has been proven to be useful in clinical ECG diagnosis. To better combine these two components, we construct a super learner to fuse what the neural network learns and what the rule inference module provides. The raw ECG signal with the gender and age information is fed to both the rule inference module and the deep learning module (see Fig. 2), and their outputs are fused by the proposed super learner for the final diagnosis prediction.

In what follows, we describe the deep learning module in Sec. III-A, the rule inference module in Sec. III-B, and the proposed super learner in Sec. III-C. The training strategy of HRNN is discussed in Sec. III-D.

A. Automatic Feature Extraction by a Deep Neural Network

As previous research has demonstrated that CNNs can well process ECG signals [13], [21], we develop an end-to-end CNN to cope with ECG signals for arrhythmia classification.

An overview of HRNN is shown in Fig. 2, in which the architecture of the CNN part (denoted by f_{CNN}) is specified in Fig. 3. This CNN architecture is modified from ResNet-34 [4]

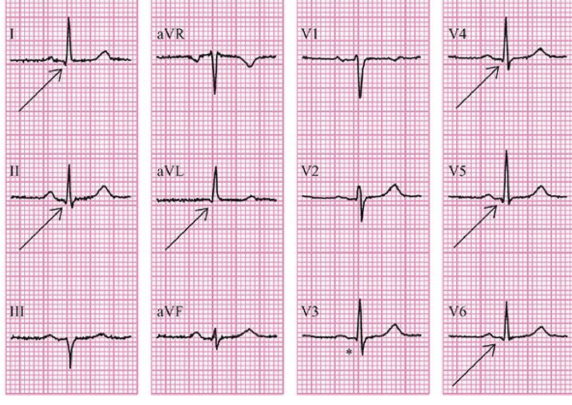


Fig. 4: A standard 12-lead ECG presented in the classical display format used in the clinical setting [37], where one fine grid (1mm) on the vertical axis indicates 0.1mV amplitudes of the ECG signal, and the ECG recording speed is typically 25 mm (i.e., covering 2.5 fine grids along the horizon axis) per second.

for image classification. In Fig. 3, a “Conv” layer indicates a 1D convolution layer, and we use the identical mapping in the shortcut connections. The batch normalization layers and rectified linear unit (ReLU) layers are placed as in the original ResNet-34, which are not shown in Fig. 3.

The input of deep learning module includes three items: the raw ECG signal, the patient’s age (encoded as a one-hot vector of size 10), and the patient’s gender (a scalar). The deep learning module outputs a probability vector for possible abnormality classes. Specifically, the input ECG signal is specified as $x \in \mathbb{R}^{w_0 \times d_0}$, where w_0 and d_0 are the length of the signal and the number of leads, respectively. The output of f_{CNN} is $z \in \mathbb{R}^{w \times d}$, which is further fed to a global average pooling layer for global semantics abstraction. The global average pooling is utilized to compress $z \in \mathbb{R}^{w \times d}$ into $z' \in \mathbb{R}^d$. Because the patient’s age and gender also affect the diagnosis results (according to clinicians’ viewpoint), we concatenate the age feature vector and gender feature with z' , and make the prediction (denoted by a vector $h \in \mathbb{R}^N$) for abnormality categories via a fully-connected layer with a sigmoid function (see Fig. 2). We define the scalar feature of gender as: (i) if the gender is missing, it is converted to 0; (2) if the gender is “male”, it is 1; (3) if the gender is “female”, it is 2. For the feature vector of age, we assume that the patient’s age is smaller than 100, and encode the numerical age as a 10-dimensional vector. If the age is missing, the vector is filled with zeros. In all the other cases, the age vector is a one-hot vector, where a “1” in the i -th position indicates that the patient’s age is in the range of $[10(i-1), 10i]$.

Our design allows to modify f_{CNN} or replace it by other end-to-end deep learning models. For example, it is possible to add the squeeze and excitation blocks [36] to the 1D convolutional layers of our proposed f_{CNN} architecture.

B. Rule Inference Module

In clinical practice, some cardiac abnormalities can be detected by quantitative analyses, measuring, e.g., the enlarge-

ment of heart muscle, electrical conduction delay or blocks, insufficient blood flow, and death of heart muscle due to coronary thrombosis [37].

Fig. 4 gives an example for visualizing the classical display format of ECG signals¹. Some abnormalities can be detected by measurements on a single ECG recording, while other abnormalities become apparent only by observing several leads and such diagnosis can be relatively complicate. As discussed in Sec. I, neural networks might ignore some clinically useful information, and thus it is our desire to introduce the assistance of rule-based methods.

In this design, we propose a rule inference module, which performs some handcrafted rules on ECG signals to introduce certain clinical information. This rule inference module consists of a “Segmentation and Delineation” part and a “Rule Inference” part. Our “Segmentation and Delineation” part processes the ECG signals to obtain the cardiac cycles and key segments of ECG (see Fig. 5). First, we apply a band-pass (3-50Hz) filter to filter the ECG signal, so as to deburr the signal and remove the signal offsets. Second, we process R peak detection and ECG segmentation. There are methods available in BioSPPy [38] to process the R peak detection and ECG segmentation. In this paper, we follow the work in [39], and utilize the first-order information and second-order information of the filtered ECG signal to delineate the P wave, QRS complex, and T wave. In experiments, we find that the “Segmentation and Delineation” part works well, and consequently, the exact cardiac cycles and key segments are obtained (see Fig. 6).

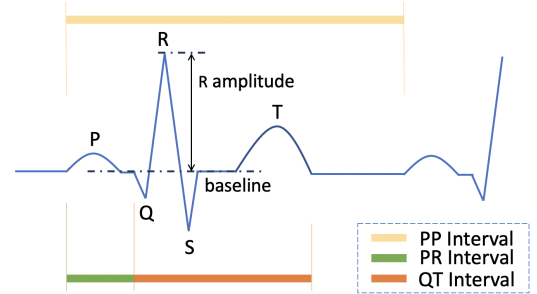


Fig. 5: An example for a single cardiac cycle of an ECG signal.

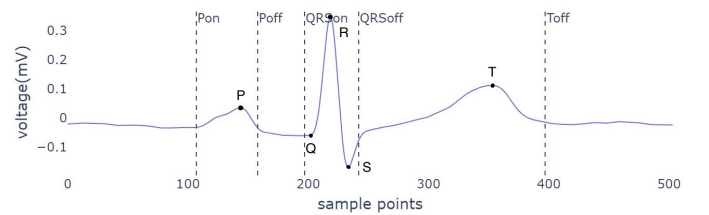


Fig. 6: An example of the segmentation and delineation results on a real ECG case.

After obtaining the cardiac cycles and key segments, we formulate rules for 15 ECG abnormalities according to criteria

¹This example is borrowed from [37].

in the previous work [37], [40], [41]. The rules are somewhat simplified, but still maintain a high degree of consistency with experts' attention on ECGs. The cardiac abnormalities measured by these rules and the corresponding rule formulas are reported in Table I, in which $t(s)$ means the duration of a segment s , $A(s|l)$ means the amplitude of a segment s in the lead l , $l \in \{I, II, III, V1-V6, aVL, aVR, aVF\}$, $v(s|l)$ indicates the voltage value of a segment s in the lead l , which is presented as a vector of the same length as a segment s , and $v(l)$ indicates the baseline voltage value of the ECG signal in the lead l . In Table I, we compute $t(s)$ (the interval time of a segment s) as in Eq. (1), where $len(s)$ is the number of the points recorded in the ECG signal, and $sr(s)$ is the sampling rate of the signal:

$$t(s) = len(s)/sr(s) \times 1000(\text{ms}) \quad (1)$$

We compute $A(s|l)$ as in Eq. (2), in which $v(l)$ means the baseline amplitude of the ECG signal. Generally, clinicians regard the 50th percentile of the voltage value of a segment from Toff to Pon as the baseline amplitude. For simplicity, $v(l)$ could be computed as 0.

$$\begin{aligned} A(s|l) &= \max((v(s|l) - v(l)) \times u)(\text{mV}), \\ &\quad \text{if } s \text{ is an "upper arch"-shaped segment} \\ &= \min((v(s|l) - v(l)) \times u)(\text{mV}), \\ &\quad \text{if } s \text{ is a "downbend"-shaped segment} \end{aligned} \quad (2)$$

where u is the unit voltage defined in the dataset. One can see that the rules define some abnormalities in a precise quantification way. In the training and inference phases, the rule inference module is performed on ECG signals without back-propagation, and yields predictions for various abnormalities. If an ECG signal meets a rule formula, then the rule inference module returns "1" for this abnormality category, and if not, the rule inference module returns "0". The predictions for all the abnormalities are concatenated into a vector, and are forwarded for final prediction.

C. A Super Learner for Prediction Fusion

To combine the predictions provided by the rule inference module and the deep learning module, it is desirable to model the dependencies between these two methods and fuse their outputs for the final cardiac abnormality identification. Here we treat both the rule inference module and the deep neural network as meta learners, and introduce a super learner to fuse their predictions.

The concept of "super learner" was first proposed in [42], which is a weighted combination of the predictions of the meta learners. In our design, the input to the super learner is two prediction vectors produced by the deep learning module, $h_{DL} = [h_1, h_2, \dots, h_N]$, and by the rule inference module, $l_{RULE} = [l_1, l_2, \dots, l_N]$, where N is the number of abnormalities, and the value of the i -th element indicates the predicted probability of the i -th abnormality (or normality). By fusing these two predictions, the proposed Super Learner produces the final prediction vector, $\hat{y} = [\hat{y}_1, \hat{y}_2, \dots, \hat{y}_N]$. Formally, the operation of the Super Learner is defined in

Eq. (3), where w is a learnable weight vector of size N , $s(w)$ is the sigmoid function, and " \cdot " denotes the element-wise dot multiplication:

$$\hat{y} = h_{DL} \cdot s(w) + l_{RULE} \cdot (1 - s(w)) \quad (3)$$

In particular, if the rule inference module considers fewer than N kinds of abnormalities, a mask vector is constructed as $mask = [m^i]_{i=1}^N$ ($m^i \in \{0, 1\}$). If the i -th abnormality (or normality) is predicted by the rule inference module, then the i -th element $m^i = 1$; otherwise, $m^i = 0$. The learnable weight vector w is of the same length as the prediction vector produced by the rule inference module, and its elements corresponding to the predictions that are not provided by the rule inference module are padded with zeros (requiring no gradients) to align with h_{DL} . The prediction vector l_{RULE} is padded in the same way. Thus, w , l_{RULE} , and h_{DL} all have the identical size of N . The masked mechanism for the final prediction is performed as in Eq. (4), where \overline{mask} indicates to invert every element in the $mask$ vector, and " \cdot " denotes the element-wise multiplication:

$$\hat{y} = mask \cdot (h_{DL} \cdot s(w) + l_{RULE} \cdot (1 - s(w))) + \overline{mask} \cdot h_{DL} \quad (4)$$

D. Model Training

The entire framework HRNN is specified using a newly proposed loss function \mathcal{L} in the training phase. Since abnormal ECG cases are usually much fewer in the real world data (the datasets), the deep neural network part might fall into a pattern collapse and indiscriminately return "zeros" (indicating the "normality" category). Thus, in designing the loss function, we manage to use the predictions generated by the rule inference module to guide the predictions of the deep learning module, because the rule inference module often performs better on the categories with fewer cases in the datasets.

Assume that the ground truth of an ECG record is $y = \{y^i\}_{i=1}^N$, $y^i \in \{0, 1\}$. When $y^i = 1$, it means that the ECG record is with the abnormality of category i , and $y^i = 0$ is for normality of category i . The weighted cross-entropy loss is defined by:

$$L(y, \hat{y}) = \sum_{i=1}^N w_i \cdot y^i \log \hat{y}^i + (1 - y^i) \log(1 - \hat{y}^i) \quad (5)$$

where w_i is the class weight of category i computed as $w_i = \frac{M}{M_i}$ (M is the total number of all ECG cases in the dataset and M_i is the number of cases belonging to category i), and \hat{y} is the prediction probabilities obtained by the Super Learner. The predictions of the rule inference module are also used to guide the prediction of HRNN, and its total loss function is defined by:

$$\mathcal{L} = L(y, \hat{y}) + \lambda L(l_{RULE}, \hat{y}) \quad (6)$$

where L is the weighted binary cross-entropy in Eq. (5), l_{RULE} is the output probabilities generated by the rule inference module, and λ is an importance parameter.

TABLE I: The formulas we use for identifying ECG abnormalities according to criteria in the medical literature [37], [40], [41]. $t(s)$ indicates the duration of a segment s , computed according to Eq. (1). $A(s|l)$ indicates the amplitude of a segment s in the lead l , computed according to Eq. (2).

ECG Abnormalities	Rule Formulas
Poor R-wave progression ¹	(a) $A(R V1) > A(R V2) > A(R V3) > A(R V4)$ (b) $A(R V2) > 0$ & $A(R V3) > 0$ & $A(R V1) + A(R V2) + A(R V3) < 0.2\text{mV}$
Arrhythmia	$\text{STD}(t(\text{PP})) > 120\text{ms}$ ²
Tachycardia	heart rate > 120
Bradycardia	heart rate < 60
Right axis deviation (RAD) ³	$-2 \times A(\text{QRS} \text{III}) < A(\text{QRS} \text{I}) < 0$ & $A(\text{QRS} \text{III}) > 0$
Left axis deviation (LAD)	$A(\text{QRS} \text{I}) > 0$ & $A(\text{QRS} \text{III}) < A(\text{QRS} \text{I})$
Low QRS voltage	$A(\text{QRS} l) < 0.5\text{mV}$, $l \in \{\text{I}, \text{II}, \text{III}\}$ or $A(\text{QRS} l) < 1\text{mV}$, $l \in \{\text{V1}, \text{V2}, \text{V3}\}$
QT prolongation	$t(\text{QT}) > 0.4\text{s}$ & $t(\text{QT})/(\text{heart rate})^{-1/2} > 0.43$
Clockwise rotation (CR)	$0.9 < A(R V1)/A(S V1) < 1.1$ & $0.9 < A(R V2)/A(S V2) < 1.1$
Counterclockwise rotation (CCR)	$A(R l)/A(S l) < 1$, $l \in \{\text{V1-V4}\}$
First degree atrioventricular block	$t(\text{PR}) > 200\text{ms}$
Abnormal Q waves	$A(Q l) > 1/4 \times A(R l)$, $l \in \{\text{II}, \text{III}, \text{aVF}\}$ or $t(Q) > 40\text{ms}$
T wave change (T change)	$A(T l) < 1/10 \times A(R l)$ or $A(T l) > 0.5\text{mV}$, $l \in \{\text{I}, \text{II}, \text{V2-V6}\}$
Right atrium enlargement (RAE)	$A(P l) \geq 0.15\text{mV}$, $l \in \{\text{V1}, \text{V2}\}$ & $A(P l) \geq 0.25\text{mV}$, $l \in \{\text{II}, \text{III}, \text{aVF}\}$
Left ventricular high voltage (LVHV) ⁴	(a) $A(R V5) > 2.5\text{mV}$ & $A(R V6) > 2.5\text{mV}$
	(b) $A(R V5) + A(S V1) > 4.0\text{mV}$ if (gender = male) or $> 3.5\text{mV}$ if (gender = female)
	(c) $A(R \text{I}) > 1.5\text{mV}$ or $A(R \text{aVL}) > 1.2\text{mV}$ or $A(R \text{aVF}) > 2.0\text{mV}$
	(d) $A(R \text{I}) + A(S \text{III}) > 2.5\text{mV}$

¹ (a) or (b) is sufficient to detect the Poor R-wave progression.

² STD denotes standard deviation computing.

³ $A(\text{QRS}|l) = A(Q|l) + A(R|l) + A(S|l)$

⁴ (a) or (b) or (c) or (d) is sufficient to detect the left ventricular high voltage.

IV. EXPERIMENTS

A. Datasets

We use the datasets for the first and second rounds of the contest of the Hefei Hi-tech Cup ECG Intelligence Competition² for a multi-label classification task of 55 classes and 34 classes, respectively. In clinical ECG diagnosis, clinicians often give detailed analysis with the pathogenesis and types of abnormalities. The datasets we use cover comprehensive ECG disease classes that are commonly found in clinical application scenarios. The dataset used in the first round of the contest (called ‘‘TianChi ECG dataset-1’’) contains 24,106 samples, and the second round dataset (called ‘‘TianChi ECG dataset-2’’) contains 20,096 samples. Each sample has 8 leads (I, II, V1, V2, V3, V4, V5, V6). Each sample was recorded in 10 seconds with 500 Hz sampling frequency, and the unit voltage is 4.88×10^{-3} millivolts. For these two datasets, the ECG input for f_{CNN} is with a shape of 5000×12 . Since the standard 12-lead ECG is the most commonly-used format in ECG analyses [43], we computationally added the other four leads to the original datasets following Eq. (7). An example of the input ECG is shown in Fig. 7.

$$\begin{aligned}
 v(\text{III}) &= v(\text{II}) - v(\text{I}) \\
 v(\text{aVR}) &= -(v(\text{I}) + v(\text{II}))/2 \\
 v(\text{aVL}) &= v(\text{I}) - v(\text{II})/2 \\
 v(\text{aVF}) &= v(\text{II}) - v(\text{I})/2
 \end{aligned} \tag{7}$$

The 55 cardiac abnormalities (or normalities) of TianChi ECG dataset-1 and the 34 cardiac abnormalities (or normalities) of TianChi ECG dataset-2 are shown in Table II.

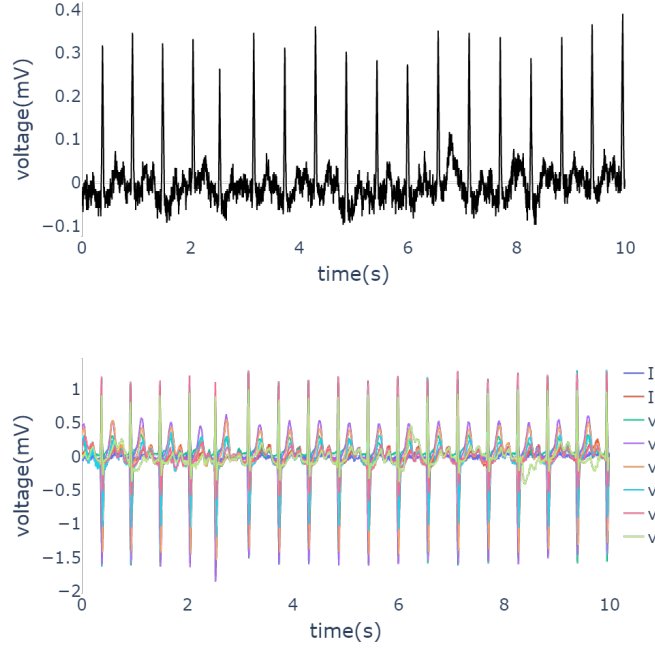


Fig. 7: An ECG signal example with lead I (top), and an ECG signal example with 8 leads (bottom).

B. Experimental Setting

We use the Adam optimizer [44] with default hyperparameters. The base learning rate (base_lr) was initialized as 10^{-4} , and we gradually warm-up [45] the first 2 epochs. The learning rate scheduler is set as the cosine scheduler with a weight decay of 10^{-6} . The batch size is 32, and the number of epochs is 60.

²<https://tianchi.aliyun.com/competition/entrance/231754/information>

TABLE II: The record number and proportion of each class in the two Tianchi ECG datasets. Some of the categories use abbreviations. The comparison table of full names and abbreviations is given in Appendix.

Categories	# of cases (proportion %)	
	ECG dataset-1	ECG dataset-2
Sinus rhythm	16918 (70.18%)	9536 (47.45%)
Bradycardia	3372 (13.99%)	5272 (26.23%)
Tachycardia	2010 (8.34%)	4910 (24.433%)
T change	3421 (14.19%)	3490 (17.37%)
RAD	1055 (4.38%)	1131 (5.628%)
LAD	1137 (4.72%)	1128 (5.613%)
Arrhythmia	924 (3.83%)	904 (4.498%)
VPB	971 (4.03%)	571 (2.841%)
RBBB	392 (1.63%)	556 (2.767%)
CRBBB	1109 (4.60%)	423 (2.105%)
LVHV	4326 (17.95%)	415 (2.065%)
APB	1470 (6.10%)	316 (1.572%)
ST-T change	2111 (8.76%)	299 (1.488%)
ST change	2967 (12.31%)	287 (1.43%)
IABV	282 (1.17%)	142 (0.707%)
IRBBB	199 (0.83%)	126 (0.627%)
Atrial fibrillation	1217 (5.05%)	120 (0.597%)
NS-ST	78 (0.32%)	64 (0.318%)
CCR	34 (0.14%)	61 (0.304%)
Abnormal Q waves	53 (0.22%)	52 (0.259%)
LABB	106 (0.44%)	36 (0.179%)
NS-T	125 (0.52%)	35 (0.174%)
CR	30 (0.12%)	35 (0.174%)
RAE	24 (0.10%)	32 (0.159%)
RVR	229 (0.95)	29 (0.144%)
LBBS	18 (0.08%)	27 (0.134%)
CLBBB	20 (0.08%)	27 (0.134%)
Short PR interval	55 (0.23%)	24 (0.119%)
Early repolarization	37 (0.15%)	22 (0.109%)
Pacing rhythm	74 (0.31%)	16 (0.08%)
Poor R-wave progression	19 (0.08%)	16 (0.08%)
NS-STT	61 (0.25%)	16 (0.08%)
Fusion wave	18 (0.08%)	8 (0.04%)
QRS low voltage	1543 (6.40%)	3 (0.015%)
Normal ECG	4171 (17.30%)	–
Critical ECG	1911 (7.93%)	–
Abnormal ECG	1061 (4.40%)	–
LVH	432 (1.79%)	–
QT prolongation	101 (0.42%)	–
Differential conduction	75 (0.31%)	–
Atrial fibrillation	42 (0.17%)	–
Intraventricular aberrant conduction	36 (0.15%)	–
Bigeminy	27 (0.11%)	–
Ventricular premature beats	33 (0.14%)	–
Abnormal repolarization	29 (0.12%)	–
uAPB	25 (0.10%)	–
Cor Pulmonale	27 (0.11%)	–
SVR	30 (0.12%)	–
Short series of atrial tachycardia	21 (0.09%)	–
RVE	18 (0.08%)	–
Atrioventricular conduction delay	10 (0.04%)	–
Bifascicular block	20 (0.08%)	–
NS-IB	17 (0.07%)	–
NS-ID	16 (0.07%)	–
P pulmonale	17 (0.07%)	–

We conduct a comprehensive evaluation, and compare our approach with four state-of-the-art ECG signal classification models, including 1D Transformer-XL [7], SE-ECGNet [46], 1D ResNet-34 [47], and MLWGAT [23], on the two TianChi ECG datasets. We adopt the same data pre-processing method and configurations for all these methods.

We develop all the models using PyTorch, and run all the experiments on an NVIDIA GTX 2080Ti 64GB GPU machine.

TABLE III: Comparison with the four state-of-the-art methods on TianChi ECG Dataset-1.

Method	OF1	CF1	OR	CR
1D Transformer [7]	0.7731	0.2814	0.7185	0.2554
1D ResNet-34 [47]	0.8679	0.4988	0.8632	0.5030
SE-ECGNet [46]	0.8651	0.5024	0.8545	0.4680
MLWGAT [23]	0.8401	0.4259	0.8267	0.3959
HRNN ¹	0.8691	0.4855	0.8653	0.4852
HRNN ²	0.6312	0.5071	0.9065	0.6318

¹With λ in Eq. (6) set to 0.

²With λ in Eq. (6) set to 1.

TABLE IV: Comparison with the four state-of-the-art methods on TianChi ECG Dataset-2.

Method	OF1	CF1	OR	CR
1D Transformer [7]	0.8950	0.3123	0.8601	0.2773
1D ResNet-34 [47]	0.9038	0.4686	0.8872	0.4598
SE-ECGNet [46]	0.9019	0.4780	0.8940	0.4620
MLWGAT [23]	0.9069	0.4883	0.8920	0.4774
HRNN ¹	0.9104	0.4655	0.9018	0.4619
HRNN ²	0.7224	0.5001	0.9520	0.6402

¹With λ in Eq. (6) set to 0.

²With λ in Eq. (6) set to 1.

C. Evaluation Metrics

Following conventional settings [21], [23] and taking patients' concern into account, we report the average per-class recall (CR), average per-class F1 (CF1), average overall recall (OR), and average overall F1 (OF1) for performance evaluation. For each ECG sample, the labels are predicted as positive if the probabilities for them are larger than 0.5. Generally, the average overall recall (OR) and average per-class recall (CR) are relatively more important for ECG abnormality detection in the clinical setting since neglecting a disease is much more harmful for the patient.

D. Experimental Results

We present comparison results with the state-of-the-art methods. In addition, we provide some running examples for showing that our model can assist detecting mislabelled samples.

1) Comparison with State-of-the-art Methods: The results of our comparative evaluation experiments are summarized in Table III and Table IV. We report the OF1, CF1, OR, and CR of the four known models evaluated on the two TianChi ECG datasets.

In Table III and Table IV, we highlight the best result for each metric in bold. One can observe from the results that our model achieves the best performance on CF1, OR, and CR. For TianChi ECG dataset-1, with $\lambda = 0$, HRNN achieves the highest OF1 score and overall recall score among all the five methods. With $\lambda = 1$, HRNN achieves a 90.7% overall recall score and a 63.2% average per-class recall score, outperforming the state-of-the-art performance by over 4% and 13%, respectively. Meanwhile, HRNN achieves a 50.7% average per-class F1 (CF1) score. For TianChi ECG dataset-2, with $\lambda = 0$, HRNN achieves the highest OF1 score and overall recall score among all the five methods. With $\lambda = 1$, HRNN achieves a 95.2% overall recall score and a

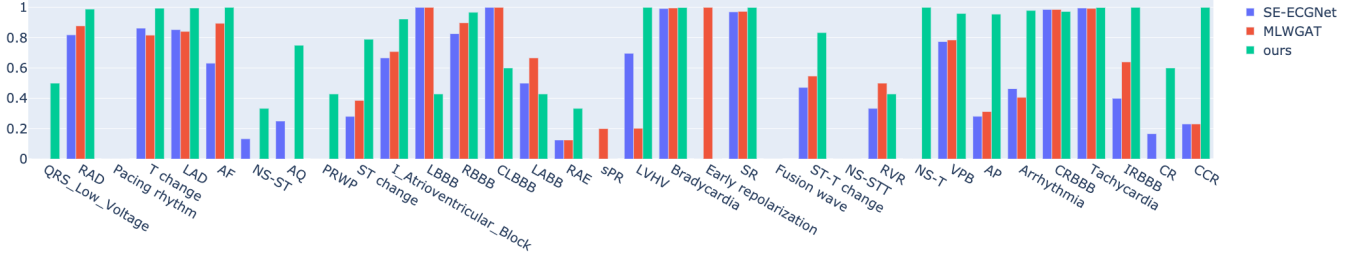


Fig. 8: Comparison of sensitivities among our proposed method and the four known state-of-the-art methods. The x -axis indicates the 34 cardiac abnormalities (or normalities) defined in TianChi ECG dataset-2, and the y -axis indicates the sensitivity (the recall score).

64.0% average per-class recall score, outperforming the state-of-the-art performance by over 5% and 16%, respectively. Meanwhile, HRNN achieves a 50.0% average per-class F1 (CF1) score and outperforms the state-of-the-art performance by 1.2%. Somehow, with $\lambda = 1$, our overall F1 (OF1) scores are lower than the four models. This is probably mainly due to the presence of more false-positive (FP) samples. False positive is a result indicating that a given condition occurs when it actually does not. If we detect FP samples, it means that our model outputs 1 for a specific disease but the ground truth of this disease is 0. However, we will show below that our identification of some of the FP samples is correct, and hence our OF1 score could be better in real settings. Also, considering the OF1 score and CF1 score at the same time, our model has a comparable or even better ability to perform multi-label classification, thus this decrease in OF1 score could be acceptable.

We also display the Recall Score (sensitivity) for each class of Tianchi ECG dataset-2 in Fig. 8. HRNN yields relatively high sensitivity in identifying different ECG abnormalities compared to the two state-of-the-art methods. In addition, we can see that there are some categories which are not included in our rule inference module, and their sensitivities still get improved (e.g., AF, NS-ST, AQ, ST-change, etc). It might be because our model gives confidence in the rule inference module, and then back-propagation pushes the deep learning module to pay more attention to the performance of the other categories. This evidence shows that our fusion of the rule inference and deep learning network outputs is effective.

Notably, we observe that 1D ResNet-34 can also attain competitive performances on TianChi ECG Dataset-1 (see Table III), but as Fig. 1 shows, the model cannot focus on the segment associated with the corresponding ECG abnormality. This might be because the deep learning model is effective for the ECG cases with obvious abnormalities, but for those abnormalities that are inconspicuous (e.g., those abnormalities that can only be observed with partial voltages and intervals), the deep learning model fails to capture accurate information. This phenomenon suggests that incorporating clinical knowledge into deep learning may provide a good potential to obtain performance improvements.

TABLE V: Ablation study on Tianchi ECG Dataset-1.

Method	OF1	CF1	OR	CR
HRNN.dl ¹ (original)	0.8661	0.4973	0.8579	0.4853
HRNN.dl ²	0.8741	0.5062	0.8743	0.4854
HRNN ($\lambda = 0$)	0.8691	0.4855	0.8653	0.4852
HRNN ($\lambda = 1$)	0.6312	0.5071	0.9065	0.6318

¹Only deep learning module in HRNN without coding information of gender and age.

²Only deep learning module in HRNN with coding information of gender and age.

TABLE VI: Ablation study on Tianchi ECG Dataset-2.

Method	OF1	CF1	OR	CR
HRNN.dl ¹ (original)	0.9033	0.4667	0.8890	0.4581
HRNN.dl ²	0.9132	0.4718	0.8981	0.4537
HRNN ($\lambda = 0$)	0.9104	0.4655	0.9018	0.4619
HRNN ($\lambda = 1$)	0.7224	0.5001	0.9520	0.6402

¹Only deep learning module in HRNN without coding information of gender and age.

²Only deep learning module in HRNN with coding information of gender and age.

2) *Ablation Studies:* We conduct experiments to verify the effect of introducing age and gender information to the neural network. We also conduct experiments to verify the contributions of the rule inference module, where we remove the meta-learner of the “Rule Inference” on the basis of HRNN and find out how the model performs. Table V and Table VI show that the information of age and gender benefits our model, which is consistent with the previous medical observations. For instance, human’s heart rate decreases with age, and the left atrial hypertrophy is also observed to be related to gender. The results in Table V and Table VI also show that our rule inference module facilitates ECG abnormality identification with a clear margin (shown by the indicators OR and CR scores).

In addition, we observe that equipping the rule inference module is almost free of cost for inference. Hence, it is promising to equip other neural networks with the rule inference module, which can improve performances at low cost.

3) *Detection of Mislabelled Samples:* Our rule inference module is able to detect mislabelled samples, as reviewed and verified by senior certified ECG clinicians. In the following examples, dash lines delineate P wave in the ECG signals, dot

lines for QRS complex, and dash-dot lines for T wave. We also add blue to the signals to illustrate the sections focused by senior certified ECG clinicians.

- Low QRS voltage: In Fig. 9, we can see that QRS amplitude is less than 5mV in limb leads, which meets the requirement according to Table I.
- Right atrium enlargement (RAE): In Fig. 10, Right atrium enlargement produces a peaked P wave (P pulmonale) with amplitude $> 0.25\text{mV}$ in the inferior leads (II, III, and AVF). However, the sample in Fig. 10 does not have a peaked P wave.
- T wave change (T change): In Fig. 11, the amplitude of the T wave is less than 1/10 of the R peak in the wave in the V1 lead.
- Right axis deviation (RAD): The sample shown in Fig. 12 meets the requirement of the corresponding rule in Table I.
- Left axis deviation (LAD): The sample shown in Fig. 13 meets the requirement of the rule for Left axis deviation in Table I.
- Counterclockwise rotation (CCR): In Fig. 14, the R wave of the V5 or V6 lead appears on the V2, V3, and V4 leads; this sample could be diagnosed as CCR.

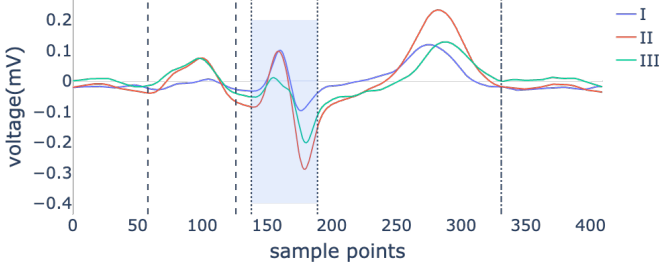


Fig. 9: Illustrating a cardiac abnormality, Low QRS Voltage, which is mislabelled as non Low QRS Voltage in the dataset.

V. CONCLUSIONS AND FUTURE WORK

In this paper, we proposed a new Handcrafted-Rule-enhanced Neural Network, HRNN, to classify arrhythmia diseases using ECG signals. To our best knowledge, this is the first approach that combines handcrafted rule methods and neural networks for multi-label ECG classification. Experiments showed that HRNN achieves the highest overall recall score and the highest average per-class recall score on both the two TianChi ECG datasets, and outperforms state-of-the-art methods with clear margins (e.g., over 4% in the overall recall score and 13% in the average per-class recall score). Meanwhile, our model attains the highest average per-class F1 score among state-of-the-art methods. Experiments also demonstrated that HRNN is able to help identify mislabelled samples, showing good potential for some practical tasks including corrupted label correction and AI-assisted annotation.

There are several possible improvements and extensions to HRNN that we would like to pursue in future work: (1)

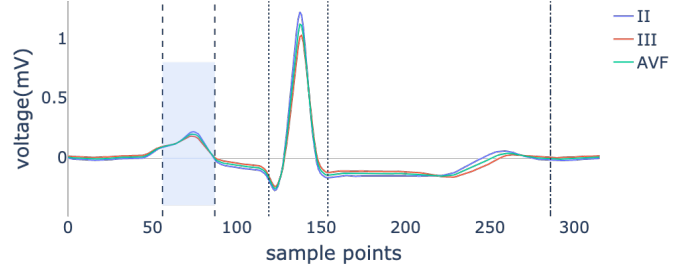
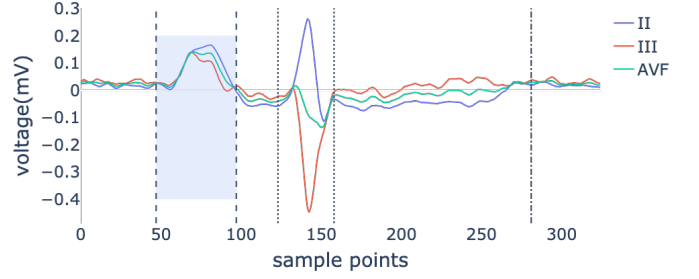


Fig. 10: An example labelled as Right atrium enlargement, which however does not have that abnormality (top); an example of RAE, mislabelled as non-RAE (bottom).

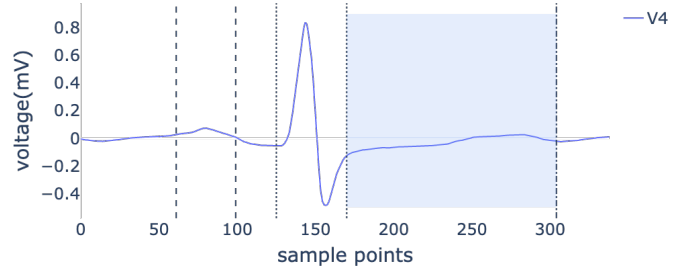


Fig. 11: An example of T wave change, mislabelled as non-T-change.

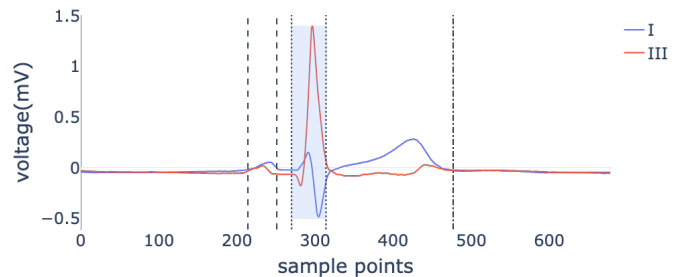


Fig. 12: An example of RAD, mislabelled as non-RAD.

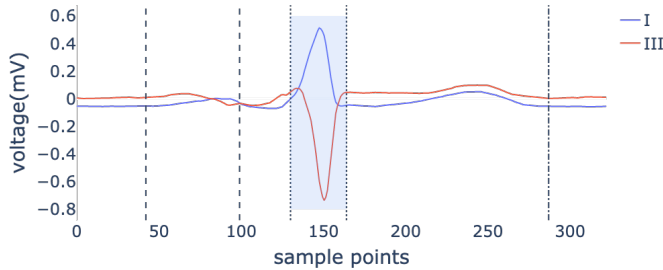


Fig. 13: An example of LAD, mislabelled as non-LAD.

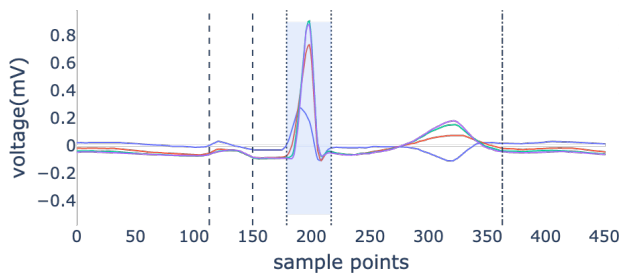


Fig. 14: An example of CCR, mislabelled as non-CCR.

encoding rules into neural networks and training rule modules with back-propagation; (2) leveraging graph neural networks to model the dependencies among different abnormalities and utilizing such dependencies in automatic ECG diagnosis.

ACKNOWLEDGMENT

This research was partially supported by National Key R&D Program of China under grant No. 2019YFB1404802, National Natural Science Foundation of China under grants No. 62176231 and 62106218, Zhejiang public welfare technology research project under grant No. LGF20F020013, Wenzhou Bureau of Science and Technology of China under grant No. Y2020082. D. Z. Chen's research was supported in part by NSF Grant CCF-1617735.

REFERENCES

- [1] H. Holst, M. Ohlsson, C. Peterson, and L. Edenbrandt, "A confident decision support system for interpreting electrocardiograms," *Clinical Physiology*, 1999. I
- [2] F. Pan, "Yuancheng xindian jiance manzu duoyanghua jiankang yiliao fuwu xuqiu-fang Zhongguo yuancheng xindianzhenduan xuezu fuzhuren Wangxinkang jiaoshou [Remote ECG monitoring meets the needs of diversified health and medical services-interview with Professor Wang Xinkang, the vice chairman of the Chinese Remote ECG Diagnostics Group]," *China Medical Herald*, 2017. I
- [3] R. R. Selvaraju, M. Cogswell, A. Das, R. Vedantam, D. Parikh, and D. Batra, "Grad-CAM: Visual explanations from deep networks via gradient-based localization," in *ICCV*, 2017. I, I
- [4] K. He, X. Zhang, S. Ren, and J. Sun, "Deep residual learning for image recognition," in *Proceedings of the IEEE Conference on Computer Vision and Pattern Recognition*, 2016, pp. 770–778. I, I, 3, III-A
- [5] K. Wei, M. Yang, H. Wang, C. Deng, and X. Liu, "Adversarial fine-grained composition learning for unseen attribute-object recognition," in *ICCV*, 2019. I

- [6] K. Wei, C. Deng, and X. Yang, "Lifelong zero-shot learning," in *IJCAI*, 2020. I
- [7] Z. Dai, Z. Yang, Y. Yang, J. Carbonell, Q. V. Le, and R. Salakhutdinov, "Transformer-XL: Attentive language models beyond a fixed-length context," *arXiv preprint arXiv:1901.02860*, 2019. I, IV-B, III, IV
- [8] K. Wei, C. Deng, X. Yang, and D. Tao, "Incremental zero-shot learning," *IEEE Transactions on Cybernetics*, 2021. I
- [9] S. Kiranyaz, T. Ince, and M. Gabbouj, "Real-time patient-specific ECG classification by 1-D convolutional neural networks," *IEEE Transactions on Biomedical Engineering*, vol. 63, no. 3, pp. 664–675, 2015. I
- [10] B. Pyakillya, N. Kazachenko, and N. Mikhailovsky, "Deep learning for ECG classification," in *Journal of Physics: Conference Series*. IOP Publishing, 2017. I
- [11] S. Saadatnejad, M. Oveis, and M. Hashemi, "LSTM-based ECG classification for continuous monitoring on personal wearable devices," *IEEE Journal of Biomedical and Health Informatics*, vol. 24, no. 2, pp. 515–523, 2019. I
- [12] J. W. Hughes, J. E. Olgin, R. Avram, S. A. Abreau, T. Sittler, K. Radia, H. Hsia, T. Walters, B. Lee, J. E. Gonzalez, et al., "Performance of a convolutional neural network and explainability technique for 12-lead electrocardiogram interpretation," *JAMA Cardiology*, 2021. I
- [13] J. Chen, H. Yu, R. Feng, D. Z. Chen, et al., "Flow-Mixup: Classifying multi-labeled medical images with corrupted labels," in *IEEE International Conference on Bioinformatics and Biomedicine*. IEEE, 2020. I, III-A
- [14] J. Chen, X. Zheng, H. Yu, D. Z. Chen, and J. Wu, "Electrocardio Panorama: Synthesizing new ECG views with self-supervision," in *IJCAI*, 2021. I
- [15] J. Rodriguez, A. Goni, and A. Illarramendi, "Real-time classification of ECGs on a PDA," *IEEE Transactions on Information Technology in Biomedicine*, 2005. I
- [16] S. Celin and K. Vasanth, "ECG signal classification using various machine learning techniques," *Journal of Medical Systems*, 2018. I
- [17] S. Ansari, N. Farzaneh, M. Duda, K. Horan, H. B. Andersson, Z. D. Goldberger, B. K. Nallamothu, and K. Najarian, "A review of automated methods for detection of myocardial ischemia and infarction using electrocardiogram and electronic health records," *IEEE Reviews in Biomedical Engineering*, 2017. I
- [18] C. Venkatesan, P. Karthigaikumar, and R. Varatharajan, "A novel LMS algorithm for ECG signal preprocessing and KNN classifier based abnormality detection," *Multimedia Tools and Applications*, 2018. I
- [19] P. Bizopoulos and D. Koutsouris, "Deep learning in cardiology," *IEEE Reviews in Biomedical Engineering*, 2018. I
- [20] S. M. Mathews, C. Kambhamettu, and K. E. Barner, "A novel application of deep learning for single-lead ECG classification," *Computers in Biology and Medicine*, 2018. I
- [21] A. Y. Hannun, P. Rajpurkar, M. Haghighpanahi, G. H. Tison, C. Bourn, M. P. Turakhia, and A. Y. Ng, "Cardiologist-level arrhythmia detection and classification in ambulatory electrocardiograms using a deep neural network," *Nature Medicine*, 2019. I, II, III-A, IV-C
- [22] C. Luo, H. Jiang, Q. Li, and N. Rao, "Multi-label classification of abnormalities in 12-lead ECG using 1D CNN and LSTM," in *Machine Learning and Medical Engineering for Cardiovascular Health and Intravascular Imaging and Computer Assisted Stenting*. Springer, 2019. I, II
- [23] H. Wang, W. Zhao, Z. Li, D. Jia, C. Yan, J. Hu, J. Fang, and M. Yang, "A weighted graph attention network based method for multi-label classification of electrocardiogram abnormalities," in *Annual International Conference of the IEEE Engineering in Medicine & Biology Society*. IEEE, 2020. I, II, IV-B, III, IV, IV-C
- [24] Z. Jiang, T. P. Almeida, F. S. Schlindwein, G. A. Ng, H. Zhou, and X. Li, "Diagnostic of multiple cardiac disorders from 12-lead ECGs using graph convolutional network based multi-label classification," in *2020 Computing in Cardiology*. IEEE, 2020, pp. 1–4. I
- [25] S. Liu, J. Shao, T. Kong, and R. Malekian, "ECG arrhythmia classification using high order spectrum and 2D graph fourier transform," *Applied Sciences*, vol. 10, no. 14, p. 4741, 2020. I
- [26] Ö. Yildirim, "A novel wavelet sequence based on deep bidirectional LSTM network model for ECG signal classification," *Computers in Biology and Medicine*, 2018. I
- [27] B. Hou, J. Yang, P. Wang, and R. Yan, "LSTM-based auto-encoder model for ECG arrhythmias classification," *IEEE Transactions on Instrumentation and Measurement*, 2019. I
- [28] J. Gao, H. Zhang, P. Lu, and Z. Wang, "An effective LSTM recurrent network to detect arrhythmia on imbalanced ECG dataset," *Journal of Healthcare Engineering*, 2019. I

- [29] Q. Yao, R. Wang, X. Fan, J. Liu, and Y. Li, "Multi-class arrhythmia detection from 12-lead varied-length ECG using attention-based time-incremental convolutional neural network," *Information Fusion*, 2020. I
- [30] Z. Zhang, J. Dong, X. Luo, K.-S. Choi, and X. Wu, "Heartbeat classification using disease-specific feature selection," *Computers in biology and medicine*, vol. 46, pp. 79–89, 2014. II
- [31] M. Xu, S. Wei, X. Qin, Y. Zhang, and C. Liu, "Rule-based method for morphological classification of ST segment in ECG signals," *Journal of Medical and Biological Engineering*, vol. 35, no. 6, pp. 816–823, 2015. II
- [32] S. Dalu and N. Pawar, "Detection and classification of qrs and st segment using wnn," *IJCSN International Journal of Computer Science and Network*, vol. 1, no. 3, 2012. II
- [33] L. Jin and J. Dong, "Classification of normal and abnormal ECG records using lead convolutional neural network and rule inference," *Science China Information Sciences*, 2017. II
- [34] G. Sannino and G. De Pietro, "A deep learning approach for ecg-based heartbeat classification for arrhythmia detection," *Future Generation Computer Systems*, vol. 86, pp. 446–455, 2018. II
- [35] V. Mondéjar-Guerra, J. Novo, J. Rouco, M. G. Penedo, and M. Ortega, "Heartbeat classification fusing temporal and morphological information of ecgs via ensemble of classifiers," *Biomedical Signal Processing and Control*, vol. 47, pp. 41–48, 2019. II
- [36] J. Hu, L. Shen, and G. Sun, "Squeeze-and-excitation networks," in *Proceedings of the IEEE Conference on Computer Vision and Pattern Recognition*, 2018, pp. 7132–7141. III-A
- [37] G. S. Wagner, *Marriott's Practical Electrocardiography*. Lippincott Williams & Wilkins, 2001. 4, III-B, 1, III-B, I
- [38] C. Carreiras, A. P. Alves, A. Lourenço, F. Canento, H. Silva, A. Fred, et al., "BioSPPy: Biosignal processing in Python," 2015. [Online]. Available: <https://github.com/PLA-Group/BioSPPy/> III-B
- [39] Y. Bian, "ECG processing: segmentation and delineation for ECG signals in Python," 2021. [Online]. Available: https://github.com/alwaysbyx/ecg_processing/ III-B
- [40] S. Kurisu, T. Iwasaki, N. Watanabe, H. Ikenaga, T. Shimonaga, T. Higaki, K. Ishibashi, Y. Dohi, Y. Fukuda, and Y. Kihara, "Poor R-wave progression and myocardial infarct size after anterior myocardial infarction in the coronary intervention era," *IJC Heart & Vasculture*, 2015. III-B, I
- [41] T. Joseph, "ECG in emergency medicine and acute care," *Emergency Medicine Australasia*, 2006. III-B, I
- [42] M. J. Van der Laan, E. C. Polley, and A. E. Hubbard, "Super learner," *Statistical Applications in Genetics and Molecular Biology*, vol. 6, no. 1, 2007. III-C
- [43] A. H. Ribeiro, M. H. Ribeiro, G. M. Paixão, D. M. Oliveira, P. R. Gomes, J. A. Canazart, M. P. Ferreira, C. R. Andersson, P. W. Macfarlane, W. Meira Jr, et al., "Automatic diagnosis of the 12-lead ECG using a deep neural network," *Nature Communications*, 2020. IV-A
- [44] D. P. Kingma and J. Ba, "Adam: A method for stochastic optimization," *arXiv preprint arXiv:1412.6980*, 2014. IV-B
- [45] P. Goyal, P. Dollár, et al., "Accurate, large minibatch SGD: Training ImageNet in 1 hour," *arXiv preprint arXiv:1706.02677*, 2017. IV-B
- [46] H. Zhang, W. Zhao, and S. Liu, "SE-ECGNet: A multi-scale deep residual network with squeeze-and-excitation module for ECG signal classification," in *IEEE International Conference on Bioinformatics and Biomedicine*, 2020. IV-B, III, IV
- [47] C. Brito, A. Machado, and A. L. Sousa, "Electrocardiogram beat-classification based on a ResNet network," in *MedInfo*, 2019, pp. 55–59. IV-B, III, IV



Yuexin Bian received her B.S. degree from Zhejiang University, China, in 2021. She is now a Ph.D. student in the Department of Electrical and Computer Engineering at University of California San Diego, USA. Her research interests include machine learning, optimization for control, data mining and signal processing and analysis. Yuexin Bian contributes to this work in Zhejiang University.



AAAI, IJCAI, IEEE TNNLS, and JBS.

Jintai Chen received the B.S. degree in applied statistics from the Zhongnan University of Economics and Law. He is currently working toward the Ph.D. degree in the College of Computer Science, Zhejiang University. His research interests includes deep learning, machine learning and data mining, especially on the computer vision, data mining, and medical intelligence. He has authored some papers at prestigious international conferences and journals, such as, ICML, AAAI, IJCAI, CVPR, MICCAI, and IEEE TMI, and served as reviewers for MICCAI,



Xiaojun Chen received the M.S. degree in applied informatics from the Liverpool University, UK, in 2017. His research interests includes machine learning, data mining, deep learning and computer vision. He has authored some papers at conferences and journals, such as, JACC and IEEE Access.



Xiaoxian Yang received the Ph.D. degree in Management Science and Engineering from Shanghai University, China, in 2017. She is currently an assistant professor at Shanghai Polytechnic University, China. Her research interests include business process management, formal verification, wireless network, and mobile health. Her researches are supported by the National Natural Science Foundation of China (NSFC), Natural Science Foundation of Shanghai (NSFS), CERNET Innovation Project, and Foundation of Science and Technology Commission of Shanghai Municipality. She has published more than 20 papers in academic journals such as TITS, TOMM, TCSS, TOIT, FGCS, MONET, IJSEKE, FGCS, IJDSN, Remote Sensing, and international conferences such as CollaborateCom, SEKE and IDEAL. She obtained 2 patents and 3 registered software copyrights in China, involving Wireless Network, Workflow Management, and Formal Verification. Dr. Yang had participated in organizing international conferences and workshops, such as CollaborateCom 2018, Chinacom 2019 and Mobicase 2019. She also worked as Guest Editor for MONET and WINE, and served as reviewers for IEEE TII, IEEE T-ITS, ACM TOMM, ACM TOIT, Wiley ETT, FGCS, PPNA, JBHI, Wireless Networks, COMPUTER NETWORK, etc.



Danny Z. Chen received the B.S. degrees in Computer Science and in Mathematics from the University of San Francisco, California, USA in 1985, and the M.S. and Ph.D. degrees in Computer Science from Purdue University, West Lafayette, Indiana, USA in 1988 and 1992, respectively. He has been on the faculty of the Department of Computer Science and Engineering, the University of Notre Dame, Indiana, USA since 1992, and is currently a Professor with tenure. Dr. Chen's main research interests include computational biomedicine, biomedical

imaging, computational geometry, algorithms and data structures, machine learning, data mining, and VLSI. He has worked extensively with biomedical researchers and practitioners, published over 150 journal papers and 240 peer-reviewed conference papers in these areas, and holds 7 US patents for technology development in computer science and engineering and biomedical applications. He received the CAREER Award of the US National Science Foundation (NSF) in 1996, a Laureate Award in the 2011 Computerworld Honors Program for developing "Arc-Modulated Radiation Therapy" (a new radiation cancer treatment approach), and the 2017 PNAS Cozzarelli Prize of the US National Academy of Sciences. He is a Fellow of IEEE and a Distinguished Scientist of ACM.



Jian Wu received the Ph.D. degree in Computer Science and Technology from Zhejiang University in 1998. He is an IEEE member, CFF member, CCF TCSC member, CCF TCAPP member and member of the "151 Talent Project of Zhejiang Province". Prof. Wu is recently the director of Research Centre of Zhejiang University and Vice-president of National Research Institute of Big Data of Health and Medical Sciences of Zhejiang University. His research interests include Medical Artificial Intelligence, Service Computing and Data Mining.